Real symmetric random matrix ensembles of Hamiltonians with partial symmetry breaking

David M. Leitner
Theoretische Chemie, Universität Heidelberg, Im Neuenheimer Feld 253, 6900 Heidelberg, Germany
(Received 9 April 1993; revised manuscript received 28 June 1993)

We investigate random matrix ensembles $E(\epsilon)$ containing real symmetric matrices $H=H^{(0)}+\epsilon V$, where $H^{(0)}$ is block diagonal, each block a member of the Gaussian orthogonal ensemble, coupled together by the Gaussian random elements of ϵV. $E(\epsilon)$ could model, for example, a chaotic Hamiltonian apart from an approximate integral of the motion. We focus on transitions in eigenvalue and eigenvector projection statistics of $E(\epsilon)$ upon variation of their respective scaling parameters. Expressions for the probability density of nearest-neighbor level spacings as well as the spectral rigidity are given, and supported by numerical data, and their application in determining a symmetry-breaking perturbation is discussed. We derive an expression for the probability density of projections of eigenvectors of $E(\epsilon)$ onto those of $E(0)$ valid for sufficiently small ϵ and use it to calculate ensemble averages and distribution functions. Each of these results is compared with numerical data. We furthermore use $E(\epsilon)$ at small ϵ to calculate average time-dependent transition probabilities of nonstationary states.

PACS number(s): 05.45.+b, 02.50.−r, 24.60.Ky

I. INTRODUCTION

Random matrix theory provides a framework to predict various properties of Hamiltonians of which our knowledge is either incomplete or which are too complicated to solve practically. Rather than solving a given Hamiltonian, one defines a matrix ensemble such that the probability density of elements therein is least biased to information available about the Hamiltonian and then calculates ensemble averages of the corresponding spectra. In the simplest case, a quantum number is taken as either totally conserved or totally nonconserved, so that the Hamiltonian is block diagonal, each block representing a set of values of the good quantum numbers. If the Hamiltonian is time-reversal invariant, the blocks are real symmetric, and ignorance of additional details about any block may be expressed by defining an ensemble of matrices whose elements are independent Gaussian random variables known as the Gaussian orthogonal ensemble (GOE) [1,2]. The GOE is furthermore ergodic, i.e., averages over the spectrum of one member of the ensemble are almost always identical to ensemble averages [3], justifying the latter procedure. The GOE has predicted energy-level statistics and spectral intensity distributions for systems where direct calculation would have otherwise been impossible. Even where is has been possible to calculate a statistical distribution of, say, level spacings from a known Hamiltonian, comparisons with the GOE have been illuminating, suggesting connections between spectral fluctuations predicted by the GOE and chaotic dynamics of autonomous, classical Hamiltonians [4].

A matrix with block-diagonal structure, each block represented by a GOE member, obtains when the Hamiltonian contains totally conserved and totally nonconserved integrals of the motion. The GOE strictly applies as a model in only this case, what Dyson [5] has referred to as its "all-or-nothing" character. More often one encounters a system in which one or more integrals of the motion are approximately conserved, whereby a different matrix ensemble is required. The investigation of one such ensemble is the topic of the following.

Modifications to the GOE accounting for approximate integrals of the motion were proposed by Dyson [5] and Rosenzweig and Porter [6] and reformulated in the context of information theory of Balian [2]. The additional constraint of an approximate integral of the motion is realized by coupling blocks belonging to different values of an approximately good quantum number by Gaussian random elements whose variance ϵ reflects the (small) symmetry breaking. Like the GOE, the modified Gaussian ensembles, which we call $E(\epsilon)$ in the following, are themselves ergodic [3].

The ensemble $E(\epsilon)$ has hereto been suggested to model symmetry breaking in both atomic and nuclear systems. In their classic study of spectra of transition metal atoms, Rosenzweig and Porter [6] observed that the energy-level statistics of the GOE alone could not account for the variety of statistics found in these atomic spectra, due to effects of spin-orbit coupling. Combining the spectra of all atoms belonging to a given period, and grouping with respect to parity, they found that the spectral statistics of each of the three periods studied may be described as follows. For one of the periods, taking total angular momentum J to be a good quantum number yields level statistics that correspond to those of the GOE. For a second period, the levels labeled again by J are described by random, Poisson statistics, at least as indicated by the nearest-neighbor level-spacings distribution. Taking spin S and orbital angular momentum L to be good quantum numbers, however, they found GOE statistics for this second period. Spectra belonging to atoms of a third period were found to be intermediate between Poisson and GOE statistics when labeled by J. To explain these findings, the authors proposed the ensemble $E(\epsilon)$, each matrix containing many blocks labeled by values of S, L, and parity. They computed numerically the probability density of nearest-neighbor level spacings, varying the

coupling parametrically. Where spin-orbit coupling is sufficiently weak, Poisson statistics are found, whereas sufficiently strong coupling brings the level statistics of $E(\epsilon)$ to the GOE limit. The third period referred to above was fit by an intermediate coupling strength.

Eigenvalue statistics of $E(\epsilon)$ have also been studied in the context of isospin symmetry breaking. Guhr and Weidenmüller [7] proposed $E(\epsilon)$ to analyze transitions in energy-level fluctuations of two isospin states with Coulomb coupling. They computed numerically the level-spacings distribution and spectral rigidity for various values of the coupling and fit them to the same level statistics obtained experimentally for the low-energy spectrum of ^{26}Al [8] to determine the strength of symmetry breaking within the errors of the latter results. In the same study, they also obtained analytical forms for level statistics of unitary ensembles, but as the unitary ensembles do not model the same problem, these expressions could not be directly compared with the experimental data.

In a recent series of studies, Bohigas and co-workers [9–11] applied ensembles similar to $E(\epsilon)$ to model systems whose classical phase-space dynamics are largely chaotic, but which also contain partial barriers to transport between chaotic regions. Members of the GOE represent the chaotic regions, their dimension corresponding to the fraction of available phase space this region represents; these are coupled by elements whose variance is related to the classical flux across a barrier. For the case of two weakly coupled regions, ensemble averages of projections of eigenvectors of $E(0)$ onto those of $E(\epsilon)$ were calculated. It was furthermore observed from this result that a wave packet initially in one region would remain localized there in the long-time limit, what was called "semi-classical" localization [11], since the corresponding classical dynamics is delocalized. The ensemble-averaged dynamics of a nonstationary state in the short- and long-time limits was calculated and compared with wave-packet dynamics using a model Hamiltonian.

As $E(\epsilon)$ has by now been applied to several problems including symmetry breaking in atoms and nuclei, as well as the semiclassical analog of classical flux across partial barriers, it is worthwhile summarizing what is known to date about $E(\epsilon)$, both from these studies and others. To our knowledge, only the work of Bohigas and co-workers [9,11] has considered eigenvector statistics of $E(\epsilon)$, referred to above. Other studies have focused on eigenvalue statistics. As demonstrated by Dyson [5], Rosenzweig and Porter [6], and most generally by Pandey [12,13], eigenvalue statistics scale with a single parameter $\Lambda \equiv \epsilon^2 D^{-2}$, where D is the local mean level spacing. Numerical studies of level-spacing statistics have been carried out with respect to Λ, for cases where $E(\epsilon)$ models a Hamiltonian with a two-value [7] and many-value [6] approximately good quantum number, as already mentioned. An approximate expression for $\Sigma^2(r;\Lambda)$, the variance of the number of levels in an interval that on average contains $r>0$ levels, was derived by French *et al.* [14]. It is expected to be most useful for spectral analysis when the number of blocks is small [14]. The number variance $\Sigma^2(r;\Lambda)$ is a two-point fluctuation measure and may be used to express any other two-point measure [3], notably the spectral rigidity $\Delta_3(r;\Lambda)$, which has been commonly applied in analyses of semiclassical spectra [15]. Numerical estimates to $\Delta_3(r;\Lambda)$, already referred to, have been given for $E(\epsilon)$ in the case of two blocks [7].

The purpose of this article is to extend the aforementioned studies of eigenvalue and eigenvector statistics of $E(\epsilon)$, focusing mainly, but not exclusively, on the small Λ regime, where expressions for eigenvalue and eigenvector statistics can be derived. If one is to determine whether a symmetry has been broken, e.g., from a sequence of energy levels, or to predict dynamics within a system where manifolds of states are weakly coupled to one another, the small Λ regime is anyway of special interest. To determine the completeness of a symmetry breaking, however, one needs eigenvalue statistics for larger Λ, and this will also be treated in the following. Comparisons with numerics are made where needed to demonstrate the range of Λ over which the following expressions are valid.

After defining $E(\epsilon)$ is Sec. II, we examine in Sec. III eigenvalue fluctuations with respect to Λ, giving expressions for the probability density of nearest-neighbor level spacings $P_S(S;\Lambda)$ and the spectral rigidity. These expressions are in part intended to complement the recent numerical analysis of these statistics for the two-block ensemble in Ref. [7]. $P_S(S;\Lambda)$ given here is valid for any number of blocks. Although it is derived assuming small Λ, we find in comparisons with numerics that it closely describes transitions with Λ nearly to the limit of the level spacings of the GOE. To determine the completeness of a symmetry breaking, we turn to a longer-range statistic $\Delta_3(r;\Lambda)$ obtained directly from $\Sigma^2(r;\Lambda)$ given by French *et al.* [14]. As the latter is expected to be most useful for only few blocks, we compare Δ_3 obtained from it with numerical results to assess its description of spectral transitions for matrices containing up to eight blocks, finding consistently good agreement. We observe furthermore that transitions of $P_S(S;\Lambda)$ and $\Delta_3(r;\Lambda)$ occur over different and complementary ranges of Λ. In analyzing a set of energy levels to determine if a symmetry is broken, $P_S(S;\Lambda)$ substantially reduces the upperbound on Λ from that obtained by $\Delta_3(r;\Lambda)$, whereas $\Delta_3(r;\Lambda)$ provides a larger lower bound on Λ, and is hence a better indicator of the completeness of a symmetry breaking.

In Sec. IV we analyze projection statistics of $E(\epsilon)$. We derive an expression for the probability density of the projection y of an eigenstate of $E(\epsilon)$, whose approximate quantum number has value b', onto an eigenstate of $E(0)$ with quantum number value $b \neq b'$. The probability density $P_y(y)$ scales with $\Lambda_b = \epsilon^2 D_b^{-2}$, where D_b is the local mean spacing of levels in block b. $P_y(y)$ given here is valid for small Λ_b. Although obtained using a series of approximations to the zero-order level spacings, we observe $P_y(y)$ to closely fit numerical results at small Λ_b over the full range of y, spanning several orders of magnitude. From $P_y(y)$ one obtains the ensemble average of y, $\langle y \rangle$, which we compare with numerical results over a wide range of values of Λ_b. Various other aspects of projec-

tion statistics, such as the distribution function of y and the dependence of $\langle y \rangle$ on the level statistics of $E(0)$, are also discussed. Finally, the average time-dependent probability of being in an eigenstate of block b for a nonstationary state starting in an eigenstate of b' is calculated using $E(\epsilon)$ and $\Lambda_b \ll 1$.

II. ENSEMBLE

The ensemble to be studied in the following, $E(\epsilon)$, contains d-dimensional real-symmetric matrices $H=H^{(0)}+\epsilon V$, where $H^{(0)}$ is block-diagonal with N blocks, each of which is a member of the GOE, and where V contains independent Gaussian random elements that couple the blocks of $H^{(0)}$. The index b labels a block and d_b is the dimension of block b. The structure of H looks like

$$H=\begin{bmatrix} H^{(0)}_{b=1} & & & \epsilon v_{ij} \\ & H^{(0)}_{b=2} & & \\ & & \ddots & \\ \epsilon v_{ji} & & & H^{(0)}_{b=N} \end{bmatrix} , \tag{1a}$$

where v_{ij} is a Gaussian random variable belonging to V. The matrix elements of H inside the block are independent Gaussian random elements with zero mean and variance

$$\langle (H_{b,ij})^2 \rangle = \tfrac{1}{2}(1+\delta_{ij})\xi_b , \tag{1b}$$

$$\xi_b = 1+\frac{\sum_{k\neq b}^{N} d_k}{1+d_b}(1-2\epsilon^2), \quad 0\le\epsilon\le 2^{-1/2} . \tag{1c}$$

The blocks are coupled to one another by elements that are also Gaussian random with zero mean and

$$\langle (H_{ij})^2 \rangle = \epsilon^2 . \tag{1d}$$

This definition of $E(\epsilon)$ was introduced by Dyson as an application of his Brownian motion model of the Gaussian ensembles and was chosen so that the variance of any eigenvalue x_i of $E(\epsilon)$ is independent of ϵ [16]. Building on the Brownian motion formalism, Pandey [12,13] showed that the energy-level statistics of $E(\epsilon)$ and a variety of other matrix ensembles scale with the local parameter

$$\Lambda(x)=\epsilon^2 D^{-2}(x) , \tag{2}$$

where D is the mean level spacing around the local energy x.

In the following, we take d_b to be large for all b, so that the level density of any block ρ_b is given by the semicircle law $\rho_b(x)=(1/\pi\xi_b)(2d_b\xi_b-x^2)^{1/2}$, $\epsilon=0$, and the total level density is $\rho(x)=\sum_b \rho_b(x)$. We will furthermore confine our numerical analysis to eigenvalues and their corresponding eigenvectors in the region $x\approx 0$ and write Eq. (2) as simply $\Lambda=\epsilon^2 D^{-2}$, where $D=\rho^{-1}(0)$.

III. EIGENVALUE STATISTICS

In this section we analyze energy-level fluctuations over short and longer energy ranges with respect to the local perturbation parameter Λ defined by Eq. (2). We begin with a short-range statistic, the probability density of nearest-neighbor level spacings $P_S(S;\Lambda)$ obtained to lowest order in Λ using degenerate perturbation theory. In the derivation we exploit an observation by Caurier, Grammaticos, and Ramani (CGR) [17], used in obtaining a distribution for the Poisson to GOE transition valid for small perturbations. As we shall see upon comparisons with numerics, $P_S(S;\Lambda)$ given here closely fits results of $E(\epsilon)$ over nearly the full transition in the spacings distribution, from $\Lambda=0$ to the GOE limit.

To determine $P_S(S;\Lambda)$, we have to consider separately the cases where nearest-neighbor levels of $H^{(0)}$ belong to the same block or to different blocks. More precisely, we write $P_S(S;\Lambda)$ as the sum of two terms

$$P_S(S;\Lambda)=P_{S,b\neq b'}(S;\Lambda)+P_{S,b=b'}(S) . \tag{3}$$

$P_{S,b=b'}(S)$ is the probability density of level spacings between nearest neighbors i and j, where $i,j\in b$, i.e., both belong to the same block of $H^{(0)}$. These levels are not affected by the perturbation to lowest order in Λ. An expression for $P_{S,b=b'}(S)$ appears in Eq. (8) below. To obtain $P_S(S;\Lambda)$ we focus now on $P_{S,b\neq b'}(S;\Lambda)$.

The perturbation calculation is done to determine $P_{S,b\neq b'}(S;\Lambda)$, the probability density of level spacings between nearest neighbors i and j, where $i\in b$, $j\in b'$, and $b\neq b'$. We consider a two-dimensional matrix whose off-diagonal elements are $\Lambda^{1/2}v$, where v is a Gaussian random variable and Λ is given by Eq. (2). The diagonal elements are $-e/2$ and $e/2$ (the trace is irrelevant to what follows, so we set it to 0), where $P_e(e)$ is the $\Lambda=0$ level-spacings distribution for i and j ($i\in b$, $j\in b'$, and $b\neq b'$), to be defined by Eq. (9) below. The level spacing S is then $S=\sqrt{e^2+4\Lambda v^2}$, and its probability density is obtained from

$$P_{S,b\neq b'}(S;\Lambda)=\int\int dv\, de\, \delta(S-\sqrt{e^2+4\Lambda v^2})P_e(e)P_v(v) . \tag{4}$$

We integrate (4) first over v, where $P_v(v)=\sqrt{(2\pi)^{-1}}e^{-v^2/2}$, then let $e=S\sin\theta$, leaving

$$P_{S,b\neq b'}(S;\Lambda)=\frac{S}{\sqrt{2\pi\Lambda}}\int_0^{\pi/2} d\theta\, e^{-S^2\cos^2\theta/8\Lambda}P_e(S\sin\theta) . \tag{5}$$

For $\Lambda\ll 1$ and $S\approx 1$, CGR have pointed out that the main contribution to the integral is where $\theta\approx\pi/2$, so that we may set $\sin\theta=1$. The integral over θ then yields

$$P_{S,b\neq b'}(S;\Lambda)=S\sqrt{\pi/8\Lambda}I_0(S^2/16\Lambda)e^{-S^2/16\Lambda}P_e(S) , \tag{6}$$

where I_0 is a Bessel function.

We still need $P_{S,b=b'}(S)$ in (3), as well as $P_e(S)$ in (6), which is the same as $P_{S,b\neq b'}(S;0)$. Both are given in Ref. [18]. They are particularly simple if we assume that the nearest-neighbor level-spacings distribution for the levels of each of the N blocks is given by the Wigner distribution

$$P_W(S)=\frac{\pi}{2}S\exp\left[-\frac{\pi}{4}S^2\right]. \tag{7}$$

Equation (7) is a very close approximation to the exact result of the GOE [1]. Using (7), one finds [18]

$$P_{S,b=b'}(S)=\frac{\pi}{2}S\left[\sum_b f_b^3\frac{e^{-(\pi/4)f_b^2S^2}}{\operatorname{erfc}\left[\frac{\sqrt{\pi}}{2}f_bS\right]}\right]\times\prod_b\operatorname{erfc}\left[\frac{\sqrt{\pi}}{2}f_bS\right], \tag{8}$$

where $f_b=d_b/d$, the fraction of levels in block b; $\operatorname{erfc}(x)=(2/\sqrt{\pi})\int_x^\infty\exp(-u^2)du$. Likewise, $P_e(S)$ is given by [18]

$$P_e(S)=\left[\left[\sum_b f_b\frac{e^{-(\pi/4)f_b^2S^2}}{\operatorname{erfc}\left[\frac{\sqrt{\pi}}{2}f_bS\right]}\right]^2-\sum_b\left[f_b\frac{e^{-(\pi/4)f_b^2S^2}}{\operatorname{erfc}\left[\frac{\sqrt{\pi}}{2}f_bS\right]}\right]^2\right]\times\prod_b\operatorname{erfc}\left[\frac{\sqrt{\pi}}{2}f_bS\right]. \tag{9}$$

This would complete the definition of $P_S(S;\Lambda)$ except for two drawbacks, namely that for $\Lambda>0$, $\int_0^\infty P_S(S;\Lambda)dS\neq1$ and $\int_0^\infty P_S(S;\Lambda)SdS\neq1$. We can get around these by introducing two parameters c_N and c_D, which are adjusted so that both of the above conditions are satisfied, i.e., $P_S(S;\Lambda)$ is normalized and $\langle S\rangle=1$. We then have

$$P_S(S;\Lambda)=c_Nc_D\sqrt{\pi/8\Lambda}I_0\left[\frac{c_D^2S^2}{16\Lambda}\right]Se^{-c_D^2S^2/16\Lambda}P_e(c_DS)+c_NP_{S,b=b'}(c_DS). \tag{10}$$

When the number of blocks is large, the second term on the right-hand side of (10) is small. Moreover, $P_e(S)$ approaches a Poisson distribution. In the large-N limit, then, we see that (10) approaches $P_S(S;\Lambda)$ given by CGR for the transition away from the Poisson distribution, apart from the additional constants we have added, c_N and c_D, for reasons discussed above.

We now test the accuracy of Eq. (10) against numerics. For illustrative purposes, we look at the two-block ensemble, studied numerically in Ref. [7]. The matrix ensembles in all our numerical tests consist of about 2000 matrices with $d=400$, $d_1=d_2=200$, from which the middle 20% of the eigenvalues of each matrix have been used for the evaluation. We can then use Eq. (2) for Λ at $x=0$ to a very good approximation. In all, we have $O(10^5)$ level spacings from each ensemble.

Figure 1 contains four plots of numerical results of $P_S(S;\Lambda)$ for $E(\epsilon)$ with $d_1=d_2=200$. The range of Λ was

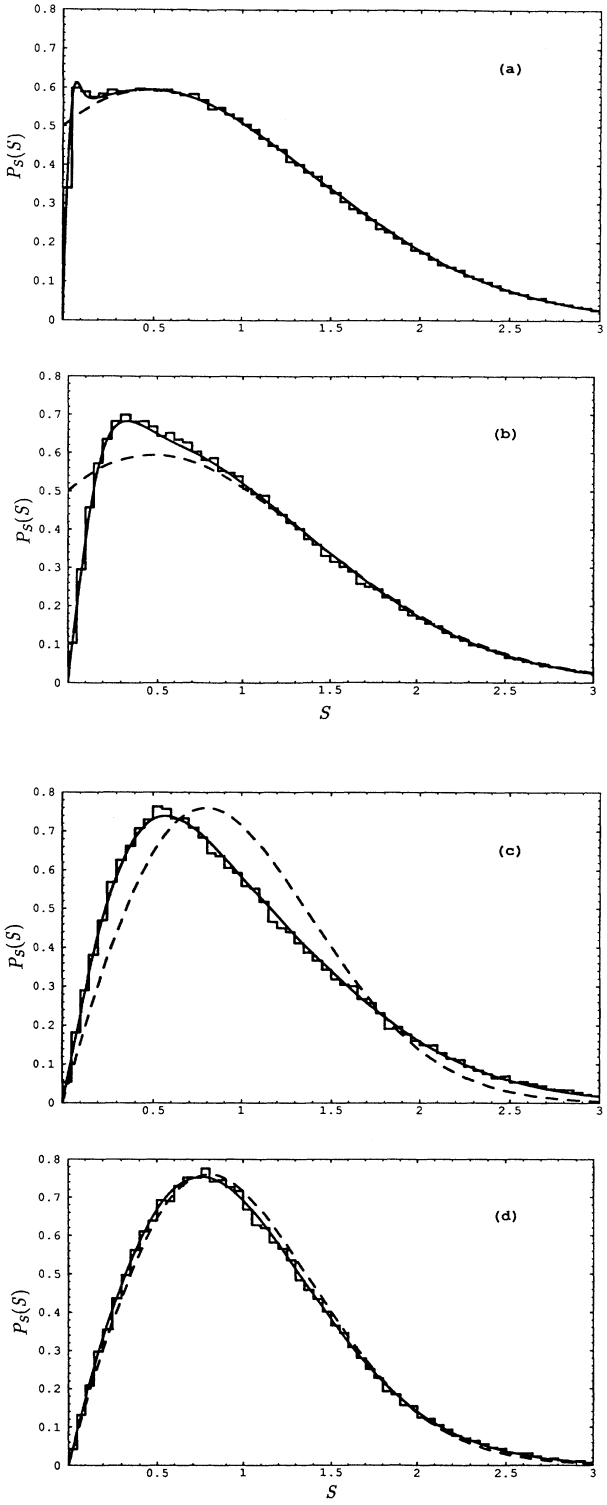

FIG. 1. $P_S(S;\Lambda)$ from Eq. (10) and numerical results for $d_1=d_2=200$, and (a) $c_N=c_D=1.000$, $\Lambda=4.05\times10^{-4}$; (b) $c_N=1.020$, $c_D=1.015$, $\Lambda=8.11\times10^{-3}$; (c) $c_N=1.125$, $c_D=1.080$, $\Lambda=4.05\times10^{-2}$; (d) $c_N=1.560$, $c_D=1.230$, $\Lambda=3.24\times10^{-1}$. The dashed line in (a) and (b) is the $P_S(S;0)$ limit, and the dashed line in (c) and (d) is the Wigner distribution, Eq. (7).

chosen so that transitions in the spacings distribution may be observed near both limits, i.e., the $\Lambda=0$ and Wigner distribution limits. We must furthermore adjust c_D and c_N in Eq. (10) with Λ to fulfill, respectively, the $\langle S\rangle=1$ and normalization requirements. In the following, we satisfy these conditions to within 1%. Since Eq. (10) then fits data where $\langle S\rangle=1$, it is necessary to "unfold" the numerical levels so that the local mean spacing is also unity.

Figure 1(a) shows both numerical results and the prediction of Eq. (10) for $\Lambda=4.05\times10^{-4}$. Here we have simply used $c_N=c_D=1$. The dashed line in the figure is the $\Lambda=0$ spacings distribution. The figure indicates close agreement between the numerically obtained histogram and the curve generated by (10). We also observe that the main difference between these and the $\Lambda=0$ spacings distribution is found at $S\approx0$. As expected from (10), $P_S(0;\Lambda\neq0)$ is 0, and for small Λ, nearly degenerate levels repel to yield slightly larger spacings, as seen by the sharp peak at $S\approx0.07$.

Figure 1(b) makes the same comparisons as 1(a), but at $\Lambda=8.11\times10^{-3}$. Level repulsion is seen to be much stronger than in 1(a), as the closely matching results of (10) and numerics differ substantially from the $\Lambda=0$ result over a range of S up to ≈1.

Figures 1(c) and 1(d) show results for Λ where $P_S(S;\Lambda)$ is converging to the Wigner distribution, Eq. (7). In 1(c) and 1(d), $\Lambda=4.05\times10^{-2}$ and 0.324, respectively. While a clear difference from the Wigner distribution is still observed in 1(c), the difference in 1(d) is small. We notice that Eq. (10), derived by perturbation theory, and numerical results agree very well as the limit of the Wigner distribution is approached. This is true in general, but somewhat more so when N is small, since small-N $P_S(S;0)$ resembles the Wigner distribution more than does $P_S(S;0)$ when N is large. Clearly we cannot determine the completeness of a symmetry breaking by looking at $P_S(S;\Lambda)$ alone. For this it is necessary to analyze alternative statistics more sensitive to long-range level fluctuations, which we turn to now.

A commonly applied long-range level statistic is the spectral rigidity, or Δ_3. As mentioned in the Introduction, Guhr and Weidenmüller [7] studied $E(\epsilon)$ numerically with $N=2$ to estimate isospin mixing in ^{26}Al by fitting the Δ_3 they obtained to that calculated from the low-energy spectrum [8], within the error bars of the data provided. Below, we consider an expression for Δ_3 obtained directly from a form for the number variance Σ^2 given by French *et al.* valid for small N [14] and compare it to numerical data.

The Δ_3 statistic was proposed by Dyson and Mehta [19] to determine the mean-square deviation from the smoothed spectral staircase and is referred to as the spectral rigidity because it shows dramatically the spectral correlation of a GOE level sequence, whose average Δ_3 rises logarithmically with the number of levels, and a random level sequence, for which Δ_3 rises linearly. Pandey [3] showed that Δ_3 is related to the number variance $\Sigma^2(r)=\langle N(r)^2\rangle-\langle N(r)\rangle^2$, where $N(r)$ is the number of levels in some length r and $\langle\ \rangle$ denote averages over a stretch of levels, or the ensemble, equivalent due to the ergodic properties of the GOE. In terms of $\Sigma^2(r)$, $\Delta_3(r)$ is [3]

$$\Delta_3(r)=\frac{2}{r^4}\int_0^r(r^3-2r^2s+s^3)\Sigma^2(s)ds\ . \tag{11}$$

For the GOE, the two-level correlation function is [19]

$$\Sigma^2(r)=\frac{2}{\pi^2}\left[\ln(2\pi r)+\gamma+1+\tfrac{1}{2}[\mathrm{Si}(\pi r)]^2-\frac{\pi}{2}\mathrm{Si}(\pi r)-\cos(2\pi r)-\mathrm{Ci}(2\pi r)+\pi^2 r\left[1-\frac{2}{\pi}\mathrm{Si}(2\pi r)\right]\right], \tag{12}$$

where Si and Ci are, respectively, the sine and cosine integrals and γ is the Euler constant.

Applying binary correlation theory [20] French *et al.* [14] obtained an expression for $\Sigma^2(r)$ valid for general Λ

$$\Sigma^2(r;\Lambda)=\Sigma^2(r;\infty)+\frac{(N-1)}{\pi^2}\ln\left[1+\frac{\pi^2r^2}{4(\tau+\pi^2\Lambda)^2}\right], \tag{13}$$

where $\Sigma^2(r;\infty)$ is the GOE limit, Eq. (12). The parameter τ is determined at $\Lambda=0$, using [3]

$$\Sigma^2(r;0)=\sum_b\Sigma^2(f_br;\infty)\ , \tag{14}$$

where $f_b=d_b/d$, the fraction of levels contained in block b. Equation (13) is valid for values of r greater than the number of blocks $r\geq N$, so we may apply it usefully for the model containing matrices with a few blocks. Using Eqs. (11) and (13), we have

$$\Delta_3(r;\Lambda)=\Delta_3(r;\infty)+\frac{(N-1)}{\pi^2}\left[\left(\frac{1}{2}-\frac{2}{\alpha^2r^2}-\frac{1}{2\alpha^4r^4}\right)\times\ln(1+\alpha^2r^2)+\frac{4}{\alpha r}\tan^{-1}(\alpha r)+\frac{1}{2\alpha^2r^2}-\frac{9}{4}\right], \tag{15}$$

$$\alpha=\frac{\pi}{2(\tau+\pi^2\Lambda)}\ ,$$

where $\Delta_3(r;\infty)$ is the GOE limit.

Figure 2 contains several plots of $\Delta_3(r;\Lambda)$ generated by Eq. (15) for the two-block ensemble $d_1=d_2$, where we use $\tau=0.70$. Six curves are plotted, which from top to bottom correspond to $\Lambda=0.0$, 0.01, 0.08, 0.24, 0.80, and ∞, respectively. For the smallest Λ represented, $\Delta_3(r;\Lambda)$ lies quite close to $\Delta_3(r;0)$. An upper bound to Λ from levels whose Δ_3 fits the $\Lambda=0$ curve would then be somewhat smaller than 0.01.

We have seen that a much smaller upper-bound to Λ can be determined from the level spacings. For example,

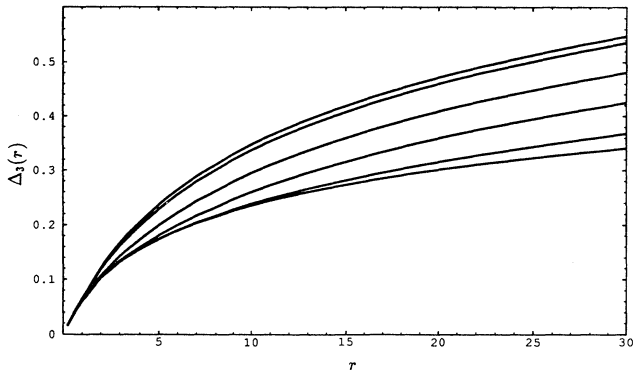

FIG. 2. $\Delta_3(r;\Lambda)$ for $d_1=d_2$ using Eq. (15) with $\tau=0.70$. From top to bottom, $\Lambda=0.00$, 0.01, 0.08, 0.24, 0.80. The bottom curve is the GOE limit $\Delta_3(r;\infty)$.

Fig. 1(a) indicates symmetry breaking at $\Lambda\approx 4\times 10^{-4}$, more than an order of magnitude smaller than the upper bound on Λ determined by Fig. 2. On the other hand, for $\Lambda=0.24$ and 0.80, the spacings distribution is close to that of the GOE limit, whereas Δ_3 for each of these parameters is clearly different from $\Delta_3(r,\infty)$. Analysis of Δ_3 thus provides a larger lower bound to Λ and is thereby a more sensitive indicator of the completeness of a symmetry breaking than $P_S(S;\Lambda)$. The main observation here is that these two statistics reveal Λ transitions in complementary intervals of Λ. The short-range $P_S(S;\Lambda)$ is most useful at small Λ, while the longer-range $\Delta_3(r;\Lambda)$ is more sensitive to larger Λ.

As remarked, Eq. (15) is most useful when N is small, since it should be valid for $r\geq N$. When N is large, French *et al.* [14] have proposed an alternative expression for $\Sigma^2(r;\Lambda)$ valid for small N, from which of course $\Delta_3(r;\Lambda)$ could be expressed. Here we test (15) to see if it is indeed useful where there are a larger number of blocks, comparing it with numerical results of an ensemble of matrices with eight blocks. Results for an ensemble of 500 matrices (the middle 20% of the eigenvalues of each matrix were used) and $d_1=\cdots=d_8=100$ are plotted in Fig. 3, together with the predictions of Eq. (15) for two values of Λ, $\Lambda=0.08$ and 0.48; $\tau=1.85$. The uppermost curve in Fig. 3 is $\Delta_3(r)=r/15$, the result for a random sequence of levels. For r to about 5, $\Delta_3(r;0)$ for $N=8$ lies close to this line, illustrating how rapidly the Poisson limit is approached with N. Each curve generated by (15) fits the numerics very closely. Some deviations are observed at small r, and for the smaller Λ also at larger r, but in both examples the dashed curves representing the numerical results follow the respective predictions of (15). For these and other cases where $N\leq 8$, we have found Eq. (15) to be a useful fit to $\Delta_3(r;\Lambda)$; we have not tested $N>8$.

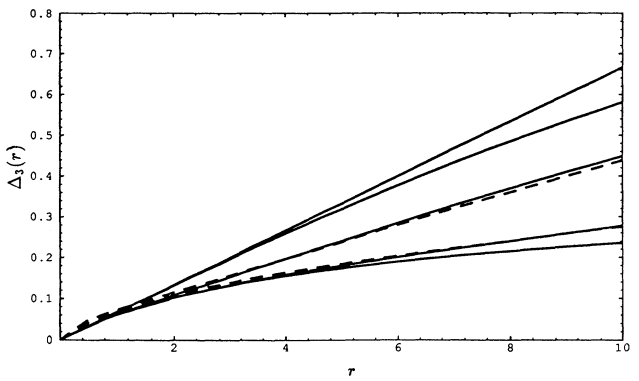

FIG. 3. $\Delta_3(r;\Lambda)$ for $N=8$ and $d_1=\cdots=d_8=100$. The dashed curves are from numerics, where $\Lambda=0.08$ and 0.48, for the upper and lower curves, respectively. The superimposed solid curves are the corresponding predictions of Eq. (15) with $\tau=1.85$. Also plotted is $\Delta_3=r/15$ (uppermost curve), the result for a sequence of random levels; the GOE limit (bottom curve); and $\Delta_3(r;0)$ for the case of eight blocks of the same dimension (second curve from top).

IV. PROJECTION STATISTICS

We now turn to transitions in the eigenstates of $E(\epsilon)$, specifically statistics of projections, y, of eigenstates of $E(\epsilon)$ with approximate quantum number value b' onto eigenstates of $E(0)$ with quantum number value $b\neq b'$. We present here an expression for the probability density of y, $P_y(y)$, which quantifies the extent of mixing of zero-order states upon introduction of the perturbation ϵ. The scaling parameter for $P_y(y)$ will be seen to be

$$\Lambda_b=\epsilon^2 D_b^{-2}\ , \tag{16}$$

where D_b is the local mean level spacing of levels in b. We approximate $P_y(y)$ by applying degenerate perturbation theory for the contributions to y from nearest-neighbor bb' levels, and nondegenerate perturbation theory and approximations to the level spacings for the rest. Despite the series of approximations required to obtain a form for $P_y(y)$, the resulting expression gives a very close fit to numerical data over the full range of y, as seen by comparison with a numerical example.

From $P_y(y)$ one may of course calculate ensemble averages of y, but only the contribution from nearest bb' levels is needed when Λ_b is sufficiently small. This was recognized by Bohigas, Tomsovic, and Ullmo [9,11] who calculated $\langle y\rangle$ for small Λ_b without first calculating $P_y(y)$, finding $\langle y\rangle=\sqrt{8/\pi}\Lambda_b^{1/2}$. One implication of this small value for $\langle y\rangle$ is that a wave packet starting in b', which is weakly coupled to the states of b, will have only a small long-time probability of being found in b, i.e., will remain localized in b', which has been called "semiclassical" localization [11].

Below we determine $P_y(y)$ and examine various aspects of projection statistics of $E(\epsilon)$. After calculating $\langle y\rangle$ from $P_y(y)$, we consider whether $\langle y\rangle$ at small Λ_b is sensitive to the level statistics of $E(0)$, comparing the cases where b' and b are members of the GOE, with that where the levels of b' and b are random. We find that to lowest order in Λ_b, $\langle y\rangle$ is the same in both cases, so that the level statistics in each of the blocks are largely irrelevant to the localization properties of the ensemble when Λ_b is small; more important are the size of the random cou-

pling elements and the level density. We then compare the lowest-order expression for $\langle y \rangle$ with $\langle y \rangle$ obtained from numerical y distributions of $E(\epsilon)$, over a wide range of Λ_b. Using $P_y(y)$, we also obtain and discuss the distribution function of y, focusing on the fraction of $P_y(y)$ found at and above $\langle y \rangle$. Finally, we examine localization properties of $E(\epsilon)$ more closely, applying the two dimensional ensemble to calculate the small-Λ_b average time-dependent probability of being in an eigenstate of b given that only a b' eigenstate is initially occupied.

Starting with the first-order, nondegenerate perturbation expression for the eigenstates, we have

$$|\tilde{i}\rangle = |i\rangle + \sum_{j\in b} \frac{v}{S_{ij}} |j\rangle \ , \tag{17}$$

where $S_{ij} \equiv E_i - E_j$, $i \in b'$, $j \in b$. The projection y of the $|j\rangle$'s onto $|\tilde{i}\rangle$ is then given by

$$y \equiv \langle \tilde{i}|\hat{P}_b|\tilde{i}\rangle = \sum_{j\in b} \frac{v^2}{S_{ij}^2} \ , \tag{18}$$

where v is a Gaussian random variable with zero mean and variance ϵ^2. To calculate the probability density of $\langle \tilde{i}|\hat{P}_b|\tilde{i}\rangle$, we need the probability densities of S_{ij}.

To simplify the notation, we define the index k, where $|k|$ ranks $|S_{ij}|$ from smallest to largest; $k=0$ corresponds to the ij pair for which $|S_{ij}|$ is smallest; $k<0$ ($k>0$) corresponds to $S_{ij}<0$ ($S_{ij}>0$). Let $\nu \equiv v^2$ and $\sigma_k \equiv S_k^2$, and define $y_k \equiv \nu/\sigma_k$. We can then express y as the sum

$$y \equiv \langle \tilde{i}|\hat{P}_b|\tilde{i}\rangle = y_0 + \sum_{k=1}^{d_b/2} (y_k + y_{-k}) \ . \tag{19}$$

Since each y_k is a random number, the probability density of y, $P_y(y)$, is the convolution of the probability densities of y_k, each k an integer between $-d_b/2$ and $d_b/2$, where d_b, the dimension of b, is assumed to be large.

For y_0, we need degenerate perturbation theory, while for y_k, $k\neq 0$, we use the nondegenerate expression. Thus we have

$$P_{y_0}(y) = \int_0^\infty \int_0^\infty \delta\left[y - \frac{1}{2}\left[1 - \left[1 + 4\frac{\nu}{\sigma}\right]^{-1/2}\right]\right] \times P_\nu(\nu) P_{\sigma_0}(\sigma) d\nu \, d\sigma \ , \tag{20a}$$

$$P_{y_k}(y) = \int_0^\infty \int_0^\infty \delta\left[y - \frac{\nu}{\sigma}\right] P_\nu(\nu) P_{\sigma_k}(\sigma) d\nu \, d\sigma \ , \quad k\neq 0 \ , \tag{20b}$$

where $P_\nu(\nu) = \sqrt{1/2\pi\epsilon^2\nu}\, e^{-\nu/2\epsilon^2}$, the Porter-Thomas distribution.

$P_{\sigma_0}(\sigma)$ is determined by $P_{S_0}(S)$, where the level spacing S_0 is the nearest-lying level of b to some level of b', b having been randomly superimposed onto b'. A derivation of the probability density of S_0 in this case is given in Refs. [18], [21], and [22]; if the nearest-neighbor level spacings of b are described by the Wigner distribution, then $P_{S_0}(S)$ is a Gaussian random variable and $P_{\sigma_0}(\sigma)$ is the Porter-Thomas distribution

$$P_{\sigma_0}(\sigma) = D_b^{-1} \sigma^{-1/2} e^{-\pi\sigma/D_b^2} \ , \tag{21}$$

where a factor 2 has been introduced to D_b^{-1} because the nearest b level may be on either side of a given b' level. Using (21) in the double integral (20a), we have

$$P_{y_0}(y) = \sqrt{2\Lambda_b/\pi}(y-y^2)^{-1/2} \times [(y-y^2)(1-8\pi\Lambda_b) + 2\pi\Lambda_b]^{-1} \ , \quad 0 \le y \le \tfrac{1}{2} \ . \tag{22}$$

It is worthwhile at this point to examine how well Eq. (22) describes the probability density of y obtained numerically. We have generated a y distribution from an ensemble of 6400 matrices, $d_{b'} = d_b = 100$ and $\epsilon = 6.32 \times 10^{-3}$. Only the middle eigenvalues were used so that $\rho_b \approx 10/\pi$. The results are plotted in Fig. 4(a), together with the corresponding prediction of Eq. (22). Close agreement is seen for larger y over a range of an order of magnitude, but is very poor at small y.

To improve our estimate to $P_y(y)$, we need to consider additional terms in (19). We do this by first assuming that for all $k\neq 0$, the probability densities of the y_k's are paired such that $P_{y_{-1}}(y) = P_{y1}(y)$, $P_{y_{-2}}(y) = P_{y2}(y)$, etc. This approximation will greatly simplify the final expression for $P_y(y)$, as we shall see below. Let l be the index corresponding to each pair, where $l = |k|$. Then

$$P_y(y) = P_{l=k=0} \circ P_{l=1} \circ P_{l=2} \cdots \ , \qquad P_l = P_{k=l} \circ P_{k=-l}, \quad l\neq 0 \tag{23}$$

where $\circ$ denotes convolution.

To solve for $P_{l=1}$ in (23), we first need to define $P_{\sigma_1}(\sigma)$ and $P_{\sigma_{-1}}(\sigma)$ to solve (20b). We guess an expression that contains both the fact that each goes to 0 as $\sigma^{1/2} \to 0$, and that the corresponding S has a mean spacing of roughly D_b. A function that satisfies both is

$$P_{\sigma_1}(\sigma) = P_{\sigma_{-1}}(\sigma) = \frac{16}{\pi^2 D_b^3} \sigma^{1/2} e^{-4\sigma/\pi D_b^2} \ , \tag{24}$$

which when transformed to $P_S(S)$ is more familiar as a close approximation to the nearest-neighbor spacings distribution of the Gaussian unitary ensemble. From (20b) and (24), we have

$$P_{|k|=1}(y) = \frac{32\sqrt{2}\Lambda_b^{3/2}}{\pi^{5/2} y^{1/2} \left[y + \frac{8}{\pi}\Lambda_b\right]^2} \ . \tag{25}$$

Using (22) and (25), we have an estimate to $P_y(y)$ that incorporates the three largest terms in the perturbation expansion (19). The resulting $P_y(y)$ is then a convolution of (25) with itself, to account for σ_1 and σ_{-1}, together with (22) to account for σ_0. In terms of index l in (23), we have so far $P_y(y) = P_{l=0} \circ P_{l=1}$. The result is plotted in Fig. 4(b), together with the same numerical results shown in 4(a). Agreement between the numerical results and our estimate to $P_y(y)$ is better than in 4(a) to an additional order of magnitude in y, i.e., $P_y(y)$ is well described

over about two orders of magnitude in y. Moreover, the fit to the smallest y's, described poorly by Eq. (22), is in much better qualitative agreement with the data.

The rest of the terms in Eq. (19) will now be included by assuming all the levels not yet accounted for are found only at intervals of D_b, or

$$P_{\sigma_{|k|}}(\sigma)=\delta(\sigma-|k|^2D_b^2) \tag{26}$$

for $|k|\geq 2$. Integration of (20b) yields

$$P_{y_{|k|}}(y)=|k|(2\pi\Lambda_b y)^{-1/2}e^{-yk^2/2\Lambda_b} . \tag{27}$$

Since $P_{y_l}=P_{y_{-k}}P_{y_k}$, we have

$$P_l(y)=l^2\Lambda_b^{-1}e^{-yl^2}\Lambda_b^{-1}, \quad l\geq 2 . \tag{28}$$

We define $P_r(y)$ as the convolution of all P_l for $l\geq 2$, and define n_l as a limit on l, which we recognize as $n_b/2$ and which can be made arbitrarily large. Then

$$P_r(y)=\left[\prod_{l=2}^{n_l}\lambda_l\right]\left[\sum_{l=2}^{n_l}B_{l,n_l}e^{-\lambda_l y}\right] ,$$

$$B_{l,n}=[(\lambda_2-\lambda_l)\cdots(\lambda_{l-1}-\lambda_l) \times(\lambda_{l+1}-\lambda_l)\cdots(\lambda_n-\lambda_l)]^{-1}, \quad 2<l<n \tag{29}$$

$$B_{n,n}=\left[\prod_{l=2}^{n-1}(\lambda_l-\lambda_n)\right]^{-1}, \quad \lambda_l=l^2\Lambda_b^{-1} .$$

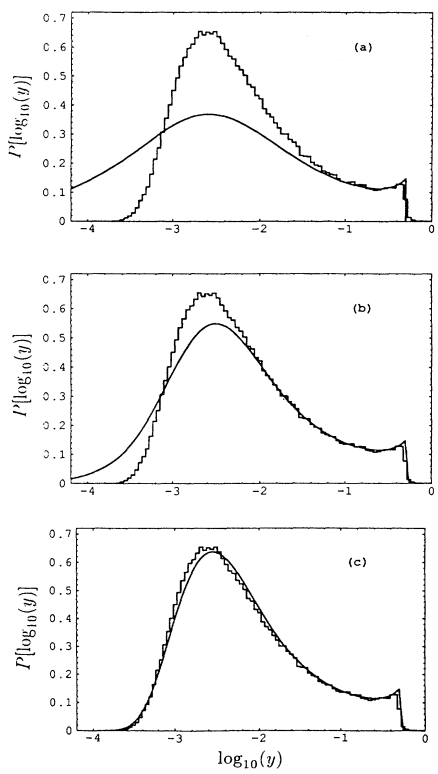

FIG. 4. (a) Histogram of $P_y(\log_{10}(y))$ obtained numerically for $d_1=d_2=100$ and $\epsilon=6.32\times10^{-3}$. The superimposed curve is the corresponding prediction of Eq. (22); (b) same as (a), but curve is the convolution of Eq. (22), (25), and (25); (c) same as (a) and (b), but curve is given by Eq. (30).

Our final expression for the probability density of y is given by

$$P_y(y)=P_{l=0}\circ P_{l=1}\circ P_r , \tag{30}$$

which is the convolution of Eqs. (22), (25), (25), and (29). Results from (30) are plotted in Fig. 4(c). Although several approximations were made in arriving at (30), the most severe ones leading to (25) and (29), the close fit to numerics over the observed range of y, more than three orders of magnitude, provides *a posteriori* justification for them.

To calculate the ensemble average of y, $\langle y\rangle$, from $P_y(y)$, only Eq. (22) is needed to lowest order in Λ_b. From (22), keeping only terms lowest order in Λ_b, we have

$$\langle y\rangle=\sqrt{8/\pi}\Lambda_b^{1/2} . \tag{31}$$

It turns out that $\langle y\rangle$ is actually insensitive to the level statistics of b and b' when Λ_b is small. To see this, we examine the extreme case for which the levels of b are random. Then

$$P_{\sigma_0}(\sigma)=D_b^{-1}\sigma^{-1/2}e^{-2\sigma^{1/2}/D_b} , \tag{32}$$

where the factor 2 appears before D_b^{-1} in the exponent as in (21). Using (31), the double integral (20a) yields

$$P_{y_0}(y)=\sqrt{2/\pi}\Lambda_b^{1/2}(y-y^2)^{-3/2}+O(\Lambda_b) , \quad 0\leq y\leq\tfrac{1}{2} , \tag{33}$$

where $O(\Lambda_b)$ contains all terms of order Λ_b or higher. To refine $P_y(y)$, we need the contribution due to the next-nearest level spacings, which for a Poisson sequence is $P_{\sigma_1}(\sigma)\propto\sigma^{1/2}e^{-2\sigma/D_b}$. Due to level repulsion between next-nearest and more distant bb' neighbors, contributions to $P_y(y)$ from these will be of order Λ_b or higher, so that to lowest order in Λ_b we have

$$P_y(y)=\sqrt{2/\pi}\Lambda_b^{1/2}(y-y^2)^{-3/2}, \quad 0\leq y\leq\tfrac{1}{2} , \tag{34}$$

and the ensemble average $\langle y\rangle=\sqrt{8/\pi}\Lambda_b^{1/2}$, the same as (31).

We now compare $\langle y\rangle$ given by Eq. (31) with numerical data to examine to what values of Λ_b and $\langle y\rangle$ this simple estimate holds. Ensembles of 1600 matrices and $d_b=d_{b'}=100$ were used, and ϵ varied over a wide range of values. The results are plotted in Fig. 5, together with the predictions of Eq. (31). In this example of two blocks of equal dimension, $\langle y\rangle$ cannot exceed 0.5; we observe that this limiting value is approached around $\Lambda_b\approx 1$, where the perturbation strength ϵ is the size of D_b. For $\langle y\rangle$ as large as 0.15, we find Eq. (31) agrees very well with numerics, to within 1%, and agrees to within 5% up to $\langle y\rangle\approx 0.25$.

We conclude this study of time-independent projection statistics by considering the distribution function of y obtained from $P_y(y)$. As is evident from Fig. 4, y extends over several orders of magnitude, and only a relatively

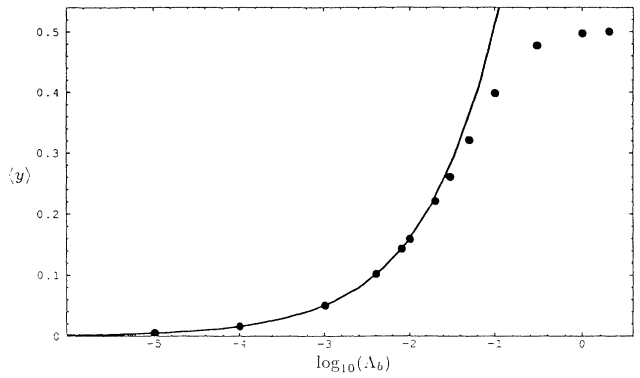

FIG. 5. Prediction of $\langle y \rangle$ given by Eq. (31) (solid curve) and $\langle y \rangle$ obtained numerically (points) at various values of $\log_{10}(\Lambda_b)$.

small fraction of all y's is observed to be around $\langle y \rangle$ or larger. We define $F_y(\langle y \rangle)$ to be the distribution function of y at $\langle y \rangle$, namely the probability that $y < \langle y \rangle$. The fraction of $y > \langle y \rangle$ is then $1-F_y(\langle y \rangle)$. Using (22), and keeping only terms lowest order in Λ_b, one obtains

$$F_y(\langle y \rangle)=1-\frac{\langle y \rangle^{1/2}(1-2\langle y \rangle)}{(1-\langle y \rangle)^{1/2}} , \tag{35}$$

which simplifies to $F_y(\langle y \rangle)=1-\langle y \rangle^{1/2}$ where $\langle y \rangle \ll 1$. This gives an indication of the spread in y, as one finds that only the fraction $\langle y \rangle^{1/2}$, or $[(8/\pi)\Lambda_b]^{1/4}$, of all y's lies at or above its ensemble average when Λ_b is small. A comparison of (35) with numerics shows agreement over the same range of Λ_b as observed for $\langle y \rangle$.

As remarked above, small $\langle y \rangle$ predicted for weakly coupled manifolds of GOE levels implies that a wave packet occupying levels of one manifold at initial time $t=0$ remains localized there in the lone-time limit. We now consider this point in more detail, calculating the average time-dependent probability $\langle P_{i\to j}(t) \rangle$ of occupying a b state starting in a b' state. We have seen that only nearest bb' states contribute to lowest order in Λ_b, so we calculate the time-dependent probability using an ensemble where $d=2$, and $i \in b'$ and $j \in b$. For this two-state problem, we have

$$|\phi(t)\rangle=\sum_{k=1,2} e^{-i\tilde{E}_k t}|\Psi_k\rangle\langle\Psi_k|i\rangle , \tag{36}$$

where $|\Psi_k\rangle$ is $|\tilde{i}\rangle$ ($|\tilde{j}\rangle$) when $k=1$ (2). Defining $P_{i\to j}(t)\equiv|\langle j|\phi(t)\rangle|^2$, and identifying $y=1-|\langle\Psi_1|i\rangle|^2$, one finds

$$P_{i\to j}(t)=4(y-y^2)\sin^2\left[\frac{\tilde{S}t}{2}\right] , \tag{37}$$

where $\tilde{S}=\tilde{E}_2-\tilde{E}_1$, and $\tilde{E}_1(\tilde{E}_2)$ is the eigenvalue corresponding to $|\tilde{i}\rangle$ ($|\tilde{j}\rangle$). For two-dimensional matrices, $\tilde{S}=\sqrt{S^2+4v^2}$, where S is the unperturbed level spacing. Using degenerate perturbation theory, we have $y=[1-(1+4v^2/S^2)^{-1/2}]/2$, so that the ensemble average of the time-dependent transition probability is

$$\langle P_{i\to j}(t)\rangle=\int_0^\infty dS\int_0^\infty dv\left[1-\left[1+4\frac{v^2}{S^2}\right]^{-1}\right]\times\sin^2\left[\frac{St}{2}\left[1+4\frac{v^2}{S^2}\right]^{1/2}\right]\times P_v(v)P_S(S) , \tag{38}$$

where $P_v(v)=\sqrt{2/\pi\epsilon^2}e^{-v^2/2\epsilon^2}$ and $P_S(S)=2D_b^{-1}e^{-\pi S^2/D_b^2}$ [see discussion up to (21)].

To lowest order in v/S, Eq. (38) is familiar as a time-dependent perturbation expression for the case where a time-independent perturbation v is switched on at $t=0$. $\langle P_{i\to j}(t)\rangle$ will clearly increase from 0 as t^2 for very small t, a dynamic that may be described as ballistic. At larger t, we expect $\langle P_{i\to j}(t)\rangle$ to enter the golden rule regime [11], i.e., depend linearly with t. One may also refer to this as a diffusive regime, where the transition rate is analogous to a diffusion constant. After very long times, the integrand in (38) oscillates very rapidly upon integration over S, leaving $\langle P_{i\to j}(t)\rangle=\pi\langle y\rangle/2$, so that for large t the wave packet is localized in b'. The latter two regimes are respectively given by

$$\langle P_{i\to j}(t)\rangle=\begin{cases}2\pi\Lambda_b D_b t \quad \text{(short times)} & \text{(39a)}\\ \sqrt{2\pi\Lambda_b}=\pi\langle y\rangle/2 \quad \text{(long times)} . & \text{(39b)}\end{cases}$$

We notice that the diffusive and saturation regimes scale differently from one another. Whereas $\langle P_{i\to j}(t)\rangle$ scales as Λ_b in the asymptotic region, it scales as $\Lambda_b D_b$ in the linear regime. This means that if we scale $\langle P_{i\to j}(t)\rangle$ in the diffusive regime, i.e., to $\Lambda_b D_b$, the long-time limit of $\langle P_{i\to j}(t)\rangle$ increases with the level density of b by a factor of $D_b^{-1/2}$ when Λ_b is small. This relation cannot, of course, be valid for all Λ_b since at some point there is complete delocalization, probably at $\Lambda_b \approx 1$. How large Λ_b can be for this relation to be valid is indicated by Fig. 5, which suggests Λ_b up to ≈ 0.03.

We integrate Eq. (38) numerically over v and S, and scale $\langle P_{i\to j}(t)\rangle$ in the golden rule regime, defining $\tau \equiv t\Lambda_b D_b$. Results for $D_b^{-1}=4.50$ and $\Lambda_b=$ (i) 5.0×10^{-7}, (ii) 1.0×10^{-6}, (iii) 2.0×10^{-6}, (iv) 4.0×10^{-6}, and (v) 8.0×10^{-6} are plotted in Fig. 6. Linear dependence of $\langle P_{i\to j}(t)\rangle$ with τ is observed at small τ, falling on the line $\langle P_{i\to j}(t)\rangle=2\pi\tau$, Eq. (39a). At even shorter times we find a quadratic dependence with τ, but this occurs over too small a range of τ to be seen in the figure (below $\tau\approx10^{-5}$). There is no apparent critical time at which $\langle P_{i\to j}(t)\rangle$ saturates to its limiting value, but rather a smooth approach over a broad range from the linear regime to the asymptotic value $\pi\langle y\rangle/2$. The conclusion drawn above is clearly shown in the figure, i.e., for a given golden rule rate, we observe always more delocalization in the long-time limit as the level density of b increases.

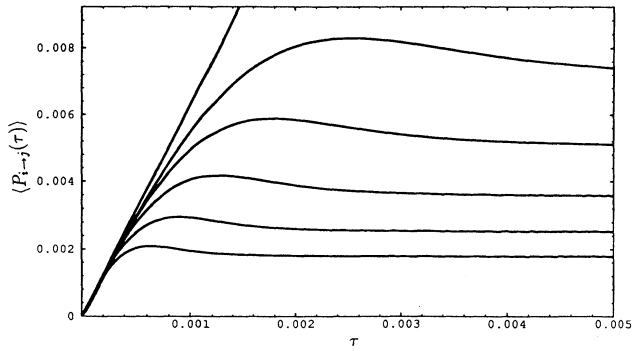

FIG. 6. $\langle P_{i\to j}(t)\rangle$ vs $\tau = t\Lambda_b D_b$, obtained by numerical integration of Eq. (38) for $D_b^{-1}=4.50$ and $\Lambda_b = 5\times10^{-7}$, 1×10^{-6}, 2×10^{-6}, 4×10^{-6}, and 8×10^{-6} (from bottom to top). The straight line is the transition probability given by (39a).

V. CONCLUSIONS

We have investigated various predictions of an ensemble $E(\epsilon)$ of real-symmetric matrices $H=H^{(0)}+\epsilon V$, where $H^{(0)}$ is block diagonal, each block a number of the GOE, coupled together by the Gaussian random elements of ϵV. The blocks of $H^{(0)}$ may be labeled by values of the good quantum numbers of $H^{(0)}$; then ϵV is related to the strength of a symmetry-breaking perturbation [2,5,6,7]. The ensemble may also model systems whose corresponding classical dynamics is characterized by a partial barrier to transport between two chaotic regions of the phase space; then the fraction of levels contributed by each block is proportional to the phase-space fraction each of the chaotic regions occupies, and the perturbation matrix reflects the classical flux across the barrier [9–11].

This study has been divided into two main areas. The first focuses on the analysis of energy-level sequences. We investigated level fluctuations over short and longer ranges of energy with respect to variation of the local perturbation parameter Λ, defined by Eq. (2). The shortest range considered was the spacing between nearest-neighbor levels. An expression was given for the probability density of nearest-neighbor spacings $P_S(S;\Lambda)$ and found to describe very closely numerical results for the ensemble over a range of Λ approaching the limit of the Wigner distribution. This is apparently because $P_S(S;\Lambda)$ comes quite close to the Wigner distribution already in the perturbation regime and is undoubtedly one reason the Wigner distribution perturbation is so often observed in spectral analyses, as it would be even in cases where the underlying Hamiltonian contains approximate integrals of the motion.

Transitions in statistics over longer-energy ranges were studied by evaluating the spectral rigidity, or Δ_3 statistic, obtained from an expression for the number variance by French *et al.* [14] valid for general Λ and small block number N. This expression has been compared with Δ_3 obtained numerically, with close agreement for $H^{(0)}$ containing up to eight blocks. Transitions in $P_S(S;\Lambda)$ and Δ_3 occur in largely different and complementary ranges of Λ. $P_S(S;\Lambda)$ yields a much lower upper bound to a symmetry-breaking perturbation than $\Delta_3(r;\Lambda)$, whereas the latter is a more sensitive indicator of the completeness of a symmetry breaking.

The second part of the study involves statistics of the eigenstates of the ensemble. We derived an expression for the probability density of the projection y of an eigenstate of $E(\epsilon)$, whose approximate quantum number has value b', onto eigenstates of $E(0)$ with value $b\neq b'$. The probability density of y, $P_y(y)$, was obtained from a full perturbation expansion and some approximations to the zero-order eigenvalue spacings and is valid when the scaling parameter Λ_b, defined by Eq. (16), is small. Despite the approximations, the fit of $P_y(y)$ to numerical results is very close over the full range of y. Various statistics obtained from $P_y(y)$, such as the distribution function of y, and the ensemble average $\langle y\rangle$ were also calculated and compared with numerics.

We furthermore studied the average time-dependent probability for a state starting in an eigenstate of block b' to be in eigenstates of b for small Λ_b. Here we observed four dynamical regimes: a ballistic at very short times; a diffusive, or golden rule regime at short times; a saturation regime at long times; and a transition regime between the latter two. The long-time saturation of the transition probability is $(\pi/2)\langle y\rangle$, and scales as Λ_b, whereas the diffusive rate scales as $\Lambda_b D_b$. For a given diffusion rate from b' to b and small Λ_b, a wave packet becomes more delocalized at long times with increasing level density of b by the factor $D_b^{-1/2}$.

Although $E(\epsilon)$ has been defined by Eq. (1) so that $H^{(0)}$ may contain any number of blocks N, it is perhaps most useful as a model when N is small. This is because for large N the level statistics are very close to Poisson statistics, and in this limit the analysis may be simplified by defining another ensemble $E_P(\epsilon)$, the same as $E(\epsilon)$, but where $H^{(0)}$ is simply diagonal. In this case, the probability density of nearest-neighbor level spacings for any value of the coupling strength ϵ has been given for the two-dimensional ensemble [23], where it is observed to fit ensembles of large matrices very satisfactorily. As mentioned above, a small-Λ expression for the number variance has also been given for $E_P(\epsilon)$ [14]. Projection statistics of $E_P(\epsilon)$ have also been analyzed and found to scale differently from the eigenvalue statistics [24], a property that is also revealed by a perturbation analysis of $E_P(\epsilon)$. An alternative description of Poisson to GOE statistics is given by an ensemble of banded matrices [25]. Indeed the banded matrix ensemble resembles more closely than $E(\epsilon)$ or $E_P(\epsilon)$ the ensemble studied by Bohigas and coworkers [9–11], since in the latter each block of $H^{(0)}$ is coupled to at most only two others, giving the matrices a banded appearance when $H^{(0)}$ has sufficiently many blocks.

ACKNOWLEDGMENTS

The author is grateful to L. S. Cederbaum and H. Köppel for providing computational facilities on which much of this work was done, and to them and M. Feingold for helpful comments on the manuscript. This material is based upon work supported by the National Science Foundation under Grant No. CHE-9002637 and the Alexander von Humboldt Foundation.

[1] C. E. Porter, *Statistical Theory of Spectra: Fluctuations* (Academic, New York, 1965); M. L. Mehta, *Random Matrices and the Statistical Theory of Energy Levels* (Academic Press, San Diego, 1991); T. A. Brody, J. Flores, J. B. Frech, P. A. Mello, A. Pandey, and S. S. M. Wong, Rev. Mod. Phys. **53**, 385 (1981).
[2] R. Balian, Nuovo Cimento B **57**, 183 (1968).
[3] A. Pandey, Ann. Phys. (N.Y.) **119**, 170 (1979).
[4] O. Bohigas and M.-J. Giannoni, in *Mathematical and Computational Methods in Nuclear Physics,* edited by J. S. Dehesa, J. M. G. Gomez, and A. Polls, Lecture Notes in Physics Vol. 209 (Springer-Verlag, Berlin, 1984), p. 1; O. Bohigas, in *Chaos and Quantum Physics,* Les Houches Lectures LII, edited by M.-J. Giannoni, A. Voros, and J. Zinn-Justin (North-Holland, Amsterdam, 1991), pp. 87–199.
[5] F. J. Dyson, J. Math. Phys. **3**, 1191 (1962).
[6] N. Rosenzweig and C. E. Porter, Phys. Rev. **120**, 1698 (1960).
[7] T. Guhr and H. A. Weidenmüller, Ann. Phys. (N.Y.) **199**, 412 (1990).
[8] G. E. Mitchell, E. G. Bilpuch, P. M. Endt, and J. F. Shriner, Jr., Phys. Rev. Lett. **61**, 1473 (1988).
[9] O. Bohigas, S. Tomsovic, and D. Ullmo, Phys. Rev. Lett. **65**, 5 (1990).
[10] U. Smilansky, S. Tomsovic, and O. Bohigas, J. Phys. A **25**, 3261 (1992).
[11] O. Bohigas, S. Tomsovic, and D. Ullmo, Phys. Rep. **223**, 43 (1993).
[12] A. Pandey, Ann. Phys. (N.Y.) **134**, 110 (1981).
[13] A. Pandey, in *Quantum Chaos and Statistical Nuclear Physics,* edited by Thomas H. Seligman and Hidetoshi Nishioka, Lecture Notes in Physics Vol. 263 (Springer-Verlag, Berlin, 1986), p. 98.
[14] J. B. French, V. K. B. Kota, A. Pandey, and S. Tomsovic, Ann. Phys. (N.Y.) **181**, 198 (1988).
[15] M. V. Berry, Proc. R. Soc. London Ser. A **400**, 229 (1985).
[16] Equation (1) is an extension of the two-block matrix ensemble in Ref. [5] to N blocks.
[17] E. Caurier, B. Grammaticos, and A. Ramani, J. Phys. A **23**, 4903 (1990); see also M. Robnik, *ibid.* **20**, L495 (1987); F. Leyvraz and T. H. Seligman, *ibid.* **23**, 1555 (1990).
[18] Appendix 1 of Ref. [6].
[19] F. J. Dyson and M. L. Mehta, J. Math. Phys. **4**, 701 (1963).
[20] K. K. Mon and J. B. French, Ann. Phys. (N.Y.) **95**, 90 (1975); J. B. French, P. A. Mello, and A. Pandey, *ibid.* **113**, 277 (1978).
[21] I. I. Gurevich and M. I. Pevsner, Nucl. Phys. **2**, 575 (1957).
[22] M. V. Berry and M. Robnik, J. Phys. A **17**, 2413 (1984).
[23] G. Lenz and F. Haake, Phys. Rev. Lett. **67**, 1 (1991).
[24] G. Lenz, K. Życzkowsky, and D. Saher, Phys. Rev. A **44**, 8043 (1991).
[25] E. P. Wigner, Ann. Math. **62**, 548 (1955); **65**, 203 (1957); T. H. Seligman, J. J. M. Verbaarschot, and M. R. Zirnbauer, Phys. Rev. Lett. **53**, 215 (1984); G. Casati, F. M. Izrailev, and L. Molinari, *ibid.* **64**, 1851 (1990); T. Cheon, *ibid.* **65**, 529 (1990); M. Feingold, D. M. Leitner, and M. Wilkinson, *ibid.* **66**, 986 (1991).